Scilight

*Journal of Mechanical Engineering and Manufacturing*
https://www.sciltp.com/journals/jmem

*Communication*

Check for updates

# Parametric Analysis of Energy Consumption in the Plasma Electrolytic Oxidation (PEO) Process

Rafael Resende Lucas [1,2,*], Rogério Pinto Mota [1], Edson Cocchieri Botelho [1] and Rita de Cássia Mendonça Sales-Contini [2,3]

[1] School of Engineering and Sciences, São Paulo State University (UNESP), São Paulo 12516-410, Brazil
[2] CIDEM, ISEP, Polytechnic of Porto, Rua Dr. António Bernardino de Almeida, 4249-015 Porto, Portugal
[3] Technologycal College, São José dos Campos, Professor Jessen Vidal Centro Paula Souza, São José dos Campos 12247-014, Brazil
* Correspondence: rr.lucas@unesp.br; Tel.: +55-(12)-98120-9031

**How To Cite:** Lucas, R.R.; Mota, R.P.; Botelho, E.C.; et al. Parametric Analysis of Energy Consumption in the Plasma Electrolytic Oxidation (PEO) Process. *Journal of Mechanical Engineering and Manufacturing* **2026**. https://doi.org/10.53941/jmem.2026.100023

Received: 28 November 2025
Revised: 14 March 2026
Accepted: 9 April 2026
Published: 3 June 2026

**Abstract:** Plasma Electrolytic Oxidation (PEO) is an advanced electrochemical treatment for lightweight alloys such as Al, Ti, and Mg. It is an environmentally friendly process that utilizes silicate, aluminate, and phosphate-based electrolytes to produce oxide/ceramic coatings with superior physical and chemical properties compared to conventional techniques. Despite extensive studies on coating morphology and performance, systematic investigations into PEO parameter optimization for reducing energy consumption, a major limitation of the process, remain scarce. To address this gap, a full factorial design ($2^3$) was employed to evaluate the influence and determine optimized values of three parameters (treatment time, duty cycle, and electrolyte concentration) that minimize average power consumption. The novelty of this work lies in the quantitative demonstration that statistical modeling can disentangle the relative contributions of process variables to energy demand, offering new insights into PEO mechanisms and paving the way for more cost-efficient and sustainable applications. Average power consumption ranged from 3.68 W to 13.67 W, with lower values linked to shorter treatment times and reduced duty cycles. Analysis of variance (ANOVA) confirmed the model's statistical robustness, explaining 89.86% of the response variability with a low noise level (0.93%). Treatment time and duty cycle were the only statistically significant factors ($p < 0.05$), contributing 8.85% and 66.98%, respectively. Beyond technological relevance, these findings provide a scientific framework for understanding parameter interactions in PEO and open promising avenues for future industrial and research applications.

**Keywords:** micro-arc oxidation; statistical design; surface treatment; energy efficiency; ANOVA

## 1. Introduction

As the global population continues to grow, energy demand increases proportionally, making it essential not only to develop new sources and methods of energy generation and storage but also to design equipment with higher energy efficiency. This trend is also reflected in material processing and treatment, since the demand for materials with enhanced properties for specific applications significantly increases energy consumption, particularly in electrochemical processes. Both developed and emerging countries have undertaken numerous efforts to promote the sustainable development of new surface treatments [1,2].

Beyond equipment, vehicles have also become central targets in efforts to reduce energy consumption. Current research primarily focuses on the selection of lightweight materials, such as aluminum, titanium, and magnesium alloys, particularly in the aerospace sector, where every reduction in structural mass directly increases the capacity for fuel and payload. Among these materials, the AA2024 (Al-Cu-Mg) alloy is widely employed in aircraft due to its high mechanical strength (~435 MPa), achieved through solution heat treatment followed by quenching and artificial aging. Despite its advantageous mechanical performance, largely attributed to the formation of intermetallic phases such as Θ ($Al_2Cu$) and S ($Al_2CuMg$), this alloy is highly susceptible to localized corrosion (pitting). This vulnerability poses a significant challenge for surface engineering studies, which aim to mitigate corrosion and enhance the reliability and safety of its use in aerospace applications [3–6].

Aiming to mitigate the corrosion rate of AA2024 aluminum alloy, numerous surface treatments have been developed. Industrially, the most prevalent approach is anodization followed by sealing, a process that generates a dense oxide coating, thereby enhancing abrasion resistance and corrosion protection. Among the most effective anodization strategies are chromic acid anodization (CAA), sulfuric acid anodization (SAA), and high-voltage sulfuric acid anodization (hard coat). The chromium-based process (CAA) is often considered the most effective, as chromate ions provide active corrosion inhibition and modify the oxide's zeta potential, effectively repelling aggressive chloride ($Cl^-$) ions [7,8].

The conventional anodizing process using acidic electrolytes, particularly those containing hexavalent chromium ($Cr^{6+}$), has been progressively phased out of industrial applications due to increasing environmental and toxicological concerns. Toxicological studies have established a correlation between $Cr^{6+}$ exposure and severe reproductive toxicity, including impaired fertility in both male and female biological systems. Coupled with stringent international regulations, this has accelerated the development of alternative surface engineering technologies [8]. Therefore, new treatments have been studied and employed in a wide variety of settings, such as the use of Chromium (III) and Oxalic acids, etc. And in the 1980s, a technological innovation called Plasma Electrolytic Oxidation (PEO) emerged.

PEO is an advanced electrochemical treatment designed specifically for light alloys, including aluminum, titanium, and magnesium. This process produces an inert oxide layer on the substrate's surfaces, exhibiting improved physical and chemical characteristics when compared to coatings produced using traditional methodologies. Similar to the anodizing procedure, in which the specimen undergoing treatment functions as the anode, while the cathode is typically an inert metal such as stainless steel or platinum, PEO operates at high voltage levels ranging from 200 to 700 volts. This enables the use of environmentally benign electrolytes formulated from silicates, aluminates, phosphates, and other compounds [9,10].

Lucas et al. [11] evaluated the energy consumption of the PEO process by varying only the electrolyte concentration, using a direct current system under potentiostatic conditions, without applying statistical design methods. The authors observed that electrolytes with conductivity above 4 mS/cm led to a significant reduction in energy consumption. This behavior was attributed to the easier ignition and stabilization of plasma discharges, promoted by the enhanced ionic mobility in the electrolyte. In addition to lightweight alloys such as aluminum (Al), titanium (Ti), and magnesium (Mg), the PEO process, with its unique characteristics of thermal, chemical, and plasma interactions, also enables the treatment of copper alloys and low-carbon steel for various applications. For example, Marcuz et al. [12] treated the AISI 1020 alloy in a TaOH-rich solution for use as a medical device. Cheng et al. [13] applied the PEO treatment to T2 copper alloy (99.9% purity), using an aluminate-based electrolyte with additives such as trisodium phosphate, sodium dihydrogen phosphate, and sodium hypophosphite, to analyze the oxide layer formation mechanisms under different electrolytes.

Guo et al. [14] incorporated graphene oxide (GO) into the PEO process, reducing the current density of the system, facilitating passivation, and more easily reaching the breakdown voltage, leading to a more energy-efficient coating process. This modification shifts the discharge mechanism from the metal/oxide interface (with higher resistance) to the oxide/electrolyte interface. It also improves the physical properties of the coating, such as antifriction behavior and increased corrosion resistance.

Although PEO has advantages in terms of enhancing the properties of metals, it faces challenges such as high energy consumption. Recent studies have explored methods to mitigate this issue by reducing the dielectric breakdown voltage. Notably, Hou et al. [9] and Zhang et al. [14] demonstrated that applying a low-energy PEO process (120 V) to various alloys can improve efficiency due to the reduced electrode distance, which optimizes the electric field action. Matykina et al. [15] applied conventional anodization in a sulfuric and phosphoric acid-based solution before PEO, achieving a 57% reduction in energy consumption and a 30–40% increase in coating microhardness. Despite the development of several approaches to minimize PEO energy demand, Troughton et al. [16] reported that most of the energy supplied during treatment is dissipated as vapor at the sample surface, subsequently leading to electrolyte heating.

The optimization of the process, in addition to the electrode spacing, can be achieved by adjusting complementary parameters such as immersion time, duty cycle, electrolyte concentration, and additives that enhance the solution's conductivity. Accordingly, the present study aims to investigate the influence of three main variables (time, duty cycle, and electrolyte concentration) on the average energy consumption during the PEO process. For this purpose, the Central Composite Design (CCD) methodology was employed, which enables the development of mathematical models for each experimental condition, as well as the construction of a *Desirability* function. This approach allows the evaluation of how specific combinations of significant variables meet a predetermined power target.

Despite advances in coating morphology and anticorrosive properties, systematic investigations on the optimization of electrical parameters such as treatment time, duty cycle, and electrolyte concentration to minimize energy consumption, which is a major limitation of the PEO process, remain scarce, especially for aerospace aluminum alloys such as AA2024. This study addresses this gap by employing Central Composite Design and ANOVA to quantify the relative contributions of these parameters to average power consumption, and by developing predictive models and optimized conditions for sustainable applications. The objectives are to evaluate the statistical influence of the variables, identify low-energy configurations, and propose a framework for industrial efficiency. The experimental methodology, detailed in Section 2, uses tetraborate and KOH electrolyte under pulsed DC conditions at 25 kHz.

## 2. Methodology

### *2.1. Aluminum Alloy*

In this study, the aluminum alloy used was AA2024 (Al-Cu), with the chemical composition provided by the manufacturer being: Si (<0.5%), Fe (<0.5%), Cu (3.8–4.9%), Mn (0.3–0.9%), Cr (<0.1%), Zn (<0.25%), Ti (<0.15%), and Al (balance), since this alloy has already been used in other studies [11].

The alloy was obtained in sheet form with a thickness of 2.0 mm, and it was necessary to cut it into strips measuring 100 × 25 mm. To control the treatment area, Kapton tape was used to isolate parts of the sample, leaving an area of 7.75 $cm^2$ for treatment. The treatment area was sanded with 100# sandpaper. After, the samples were cleaned using a water and neutral detergent solution in an ultrasonic bath for 600 s, followed by cleaning with isopropyl alcohol. They were dried and stored for the PEO treatment.

### *2.2. Experimental Design of PEO Treatment*

A full factorial design 2k was employed, where k = 3 parameters: immersion time in seconds (X1), Duty Cycle in % (X2), and electrolyte concentration in g/L (X3), with the addition of central points "0" and axial "±α", which facilitate the forecasting of the characteristics of a response surface, thus delineating a central composite design (CCD), with the power consumption (W) designated as the response variable. These data points are enumerated in Table 1.

This factorial design has already been used in a previous study [17]; however, the variable response of energy consumption throughout the PEO treatment was optimized.

**Table 1.** Operational ranges and coding of process variables applied to PEO optimization.

| Real Variables | Coded | Levels | | | | |
|---|---|---|---|---|---|---|
| | | **−α** | **−1** | **0** | **+1** | **+α** |
| Time (s) | X1 | 197 | 300 | 450 | 600 | 702 |
| Duty Cycle (%) | X2 | 15 | 20 | 45 | 70 | 87 |
| Concentration (g/L) | X3 | 0.6 | 3.0 | 6.5 | 10.0 | 12.0 |

Based on the data presented in Table 1, 17 experimental runs were generated, consisting of 8 factorial points, 3 central points, and 6 axial points. For statistical analysis, Design-Expert software version 6.0.6 was used, and an analysis of variance (ANOVA) was conducted to evaluate the significance of each parameter on the response variable.

### *2.3. PEO Treatment on AA2024 Samples*

The electrolyte was prepared from sodium tetraborate ($N_{a_2}B_4O_7 \cdot 10H_2O$) at concentrations specified in Table 1, with the addition of potassium hydroxide (KOH, 1.5 g/L; 99% purity, Dinâmica Ltd.a., São Paulo, Brazil). Deionized water was used as the solvent, and after 15 min of ultrasonic agitation, the solution exhibited a pH of ~10 and a conductivity of 4630-12920 μS/cm.

The treatment system consisted of a pulsed DC power supply model PS-2 by T2S Technology (Brazil) (0–900 VDC), operating at 25 kHz and generating a square waveform with an adjustable duty cycle ranging from 15 to 100%. A 25 Ω rheostat was used for current control, and a stainless steel (AISI 304) beaker served as the cathode.

In this study, the current was maintained at approximately 60 mA, considering the treatment area (7.75 $cm^2$), resulting in a current density of 7.74 $mA/cm^2$. The distance between the sample and the cathode was set at 2 cm, as previously used in earlier studies [11,17].

## 3. Results and Discussions

### *3.1. Voltage/Time and Current Density/Time Curves in PEO Treatment*

In Figure 1, the variation in voltage and current density throughout the PEO process is observed. Since the process typically occurs in galvanostatic mode (constant current), the voltage needs to increase to maintain the current density.

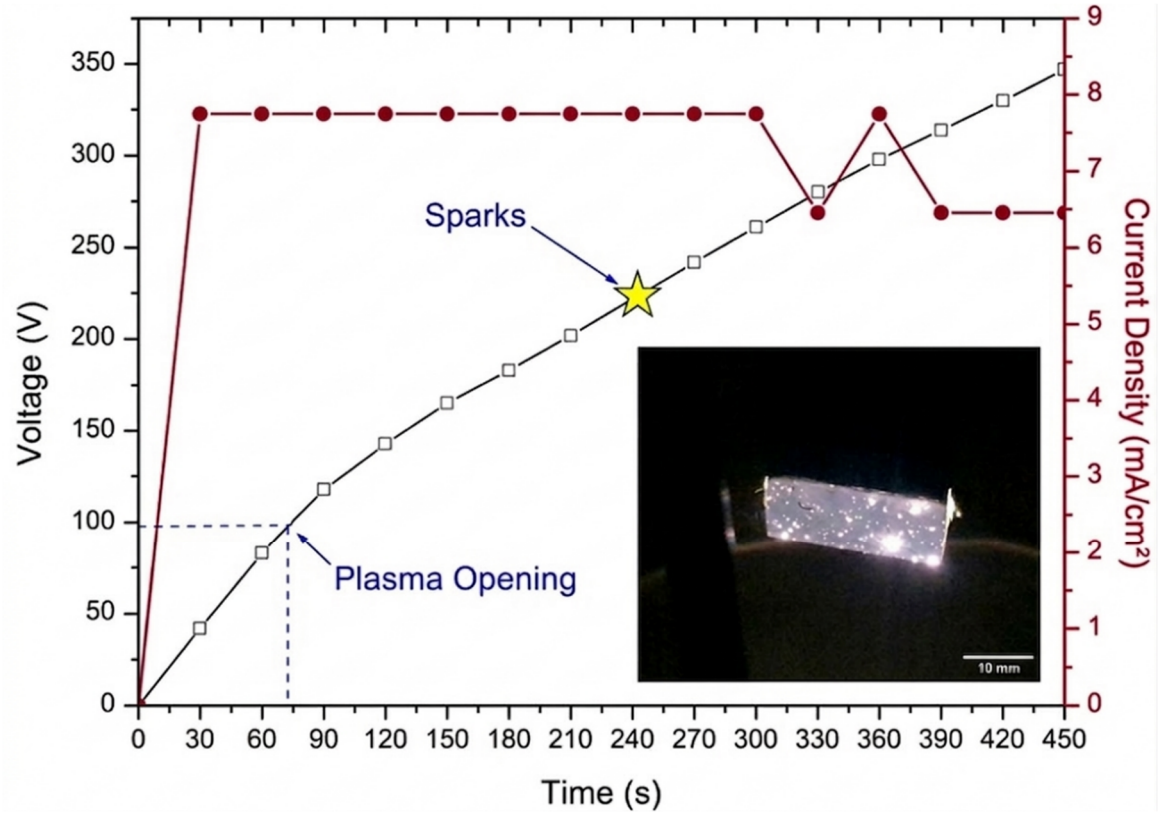


**Figure 1.** Evolution of voltage and current density throughout the PEO treatment of one sample.

Through experimental observations and the graph in Figure 1, it was observed that the treatment exhibited three stages: anodic oxidation, spark discharge, and micro-arc oxidation, as also noted by other authors [15,16,18–20].

At the beginning of the PEO treatment (0 to 70 s), a linear increase in voltage was observed at a rate of 1.43 V/s. During this period, a high concentration of bubbles around the samples was noted, but no plasma formation was observed. In the second stage, the onset of spark discharge (70 to 240 s), luminescence on the sample surface indicated the ionization of gases generated on the surface. This stage ranged from 100 V to 225 V. According to the literature, the dielectric resistance of the coating increases with the treatment time, and for the coating to develop, an increase in voltage (breakdown voltage) is required [15,16,21]. In this study, the breakdown voltage of this configuration was 225 V, with micro-arcs observed across the entire sample surface (Figure 1), followed by the characteristic crackling noise of the PEO process. This process occurred over a period of 240 to 450 s, with a final voltage of 347 V.

An interesting point to note is that around 300 s, a variation in current density occurs, despite the increase in voltage throughout the process. This can be attributed to the increase in the thickness of the alumina dielectric coating [9,19,21].

It is imperative to acknowledge that the ultimate voltage varies across processes due to alterations in process parameters (duration, Duty Cycle, and electrolyte concentration), as well as the intricate interplay among these parameters.

### *3.2. Average Power Consumed*

The system voltage and current were monitored directly on the power supply and recorded by a camera throughout the treatment. The data were then plotted every 30 s of recording. With this information, it was possible to calculate the instantaneous power. However, due to the variation in power during the treatment, it was necessary to integrate (Equation (1)) the functions corresponding to each process, as previously employed in other studies [20,21]. This was done using Excel, employing the polynomial trendline function for each plotted curve (Table 2) to estimate the average power consumed in the system.

$$P = \frac{1}{T}\int_0^T V(t)\, I(t) dt \quad (1)$$

In Equation (1), $V(t)$ and $I(t)$ represent the voltage and current signals, respectively, provided by the power supply, and $T$ is the time during which each process was conducted. Considering that the process exhibits ohmic behavior, at least in the initial stage (anodic oxidation), the ohmic resistance is lower, allowing for charge transfer between the metal/coating/electrolyte interfaces [20].

**Table 2.** Second-order polynomial equations obtained to describe the experimental response of each PEO run.

| Standard | Function—*f*(*x*) |
|---|---|
| 01 | $f(x) = -1 * 10^{-6}x^2 + 0.0325x + 0.358$ |
| 02 | $f(x) = -6 * 10^{-6}x^2 + 0.0267x + 0.435$ |
| 03 | $f(x) = -0.0001x^2 + 0.1018x + 1.398$ |
| 04 | $f(x) = -7 * 10^{-6}x^2 + 0.021x + 0.3185$ |
| 05 | $f(x) = 7 * 10^{-5}x^2 + 0.0603x + 0.8523$ |
| 06 | $f(x) = -1 * 10^{-5}x^2 + 0.0261x + 0.2759$ |
| 07 | $f(x) = -0.0002x^2 + 0.11x + 0.5392$ |
| 08 | $f(x) = -4 * 10^{-5}x^2 + 0.0535x - 0.055$ |
| 09 | $f(x) = -0.0002x^2 + 0.0748x - 0{,}017$ |
| 10 | $f(x) = -3 * 10^{-5}x^2 + 0.0436x + 0.4493$ |
| 11 | $f(x) = -2 * 10^{-5}x^2 + 0.0285x + 0.4234$ |
| 12 | $f(x) = -0.0001x^2 + 0.0847x + 1.178$ |
| 13 | $f(x) = -6 * 10^{-5}x^2 + 0.0572x - 0.0588$ |
| 14 | $f(x) = -4 * 10^{-5}x^2 + 0.0507x + 1.234$ |
| 15 | $f(x) = -6 * 10^{-5}x^2 + 0.054x + 2.1794$ |
| 16 | $f(x) = -9 * 10^{-5}x^2 + 0.0744x + 0.5232$ |
| 17 | $f(x) = -3 * 10^{-5}x^2 + 0.0429x + 0.5485$ |

After applying Equation (1) to the integrated functions in Table 2, the average powers consumed were obtained and are presented in Table 3. Since a Central Composite Design (CCD) was used in this study for (k = 3) factors, the matrix consists of three different groups of elements for experimentation: a full factorial ($2^3$) (8 experimental tests), a specified number of central points "0" (3 experimental tests), and additionally, a group of axial points "α" (6 experimental tests).

It has been noted that the power consumption values span from 3.68 W to 13.67 W (Table 3), with specific attention drawn to test number 5, which demonstrated minimal power consumption. This enhancement renders the process more appealing for both the industrial sector and academic research. Treatments characterized by a reduced Duty Cycle display diminished power consumption rates, as corroborated by findings in other scholarly investigations [20].

Longer treatment times result in higher power consumption. On average, treatments of 600 s consumed about 9.092 watts, while processes conducted for 300 s consumed approximately 8.31 watts. The Duty Cycle also has a strong influence on energy consumption. For example, comparing test 01 (4.85 watts) with test 03 (13.67 watts), it is observed that the power consumption nearly triples with a Duty Cycle of 70%. This is because the Duty Cycle affects the distribution of energy on the sample's surface, increasing the thickness of the oxide layer ($Al_2O_3$), which has dielectric properties. Consequently, the system's resistance increases, forcing it to raise the voltage to maintain a constant current, like what happens with longer oxidation times [18,22,23].

**Table 3.** Values of the operating parameters and their coded levels, along with the average electrical power consumed during the process.

| Standard | Coded Variable | | | Real Variable | | | Power (W) | Energy (kJ) |
|---|---|---|---|---|---|---|---|---|
| | X1 | X2 | X3 | Time (s) | Duty (%) | Conc. (g/L) | | |
| 01 | −1 | −1 | −1 | 300 | 20 | 3.0 | 4.85 | 1.45 |
| 02 | +1 | −1 | −1 | 600 | 20 | 3.0 | 7.73 | 4.64 |
| 03 | −1 | +1 | −1 | 300 | 70 | 3.0 | 13.67 | 4.10 |
| 04 | +1 | +1 | −1 | 600 | 70 | 3.0 | 10.54 | 6.33 |
| 05 | −1 | −1 | +1 | 300 | 20 | 10.0 | 3.68 | 1.10 |
| 06 | +1 | −1 | +1 | 600 | 20 | 10.0 | 6.91 | 4.14 |
| 07 | −1 | +1 | +1 | 300 | 70 | 10.0 | 11.04 | 3.31 |
| 08 | +1 | +1 | +1 | 600 | 70 | 10.0 | 11.20 | 6.72 |
| 09 | −α | 0 | 0 | 197 | 45 | 6.5 | 4.76 | 0.94 |
| 10 | +α | 0 | 0 | 702 | 45 | 6.5 | 10.83 | 7.60 |
| 11 | 0 | −α | 0 | 450 | 15 | 6.5 | 5.49 | 2.47 |
| 12 | 0 | +α | 0 | 450 | 87 | 6.5 | 13.49 | 6.07 |
| 13 | 0 | 0 | −α | 450 | 45 | 0.6 | 8.76 | 3.94 |
| 14 | 0 | 0 | +α | 450 | 45 | 12.0 | 9.94 | 4.47 |
| 15 | 0 | 0 | 0 | 450 | 45 | 6.5 | 10.28 | 4.63 |
| 16 | 0 | 0 | 0 | 450 | 45 | 6.5 | 11.19 | 5.04 |
| 17 | −1 | −1 | −1 | 300 | 20 | 3.0 | 4.85 | 2.18 |

Considering the energy density and the surface area of 0.000775 $m^2$, it was found that the obtained values ranged between 1.21 and 9.81 $MJ/m^2$. These results are significantly higher than those reported in the literature, such as the study by Frutuoso et al. [21], who achieved 117.8 $kJ/m^2$ using a solution of 0.25 M $Ca(CH_3COO)_2 \cdot H_2O$ and 0.025 M $NaH_2PO_4 \cdot 2H_2O$. This significant difference can be attributed to the conductivity of the electrolytes employed: while the electrolyte used by Frutuoso et al. exhibited high conductivity, in the present study, it was observed, as evidenced by the conductivity analysis (Figure 2), that the sodium tetraborate solution with KOH addition is considerably less conductive. This characteristic justifies the need for higher energy consumption to carry out the treatments, resulting in values far above those previously reported [20]. Furthermore, it is noted that, with increasing concentration, conductivity rises significantly only at higher concentrations (10 g/L), a behavior that is directly reflected in power consumption. This effect highlights the strong influence of electrolyte composition on plasma initiation and stability, as well as on the overall energy demand of the process, which explains the differences observed when compared with electrolytes traditionally reported in the literature.

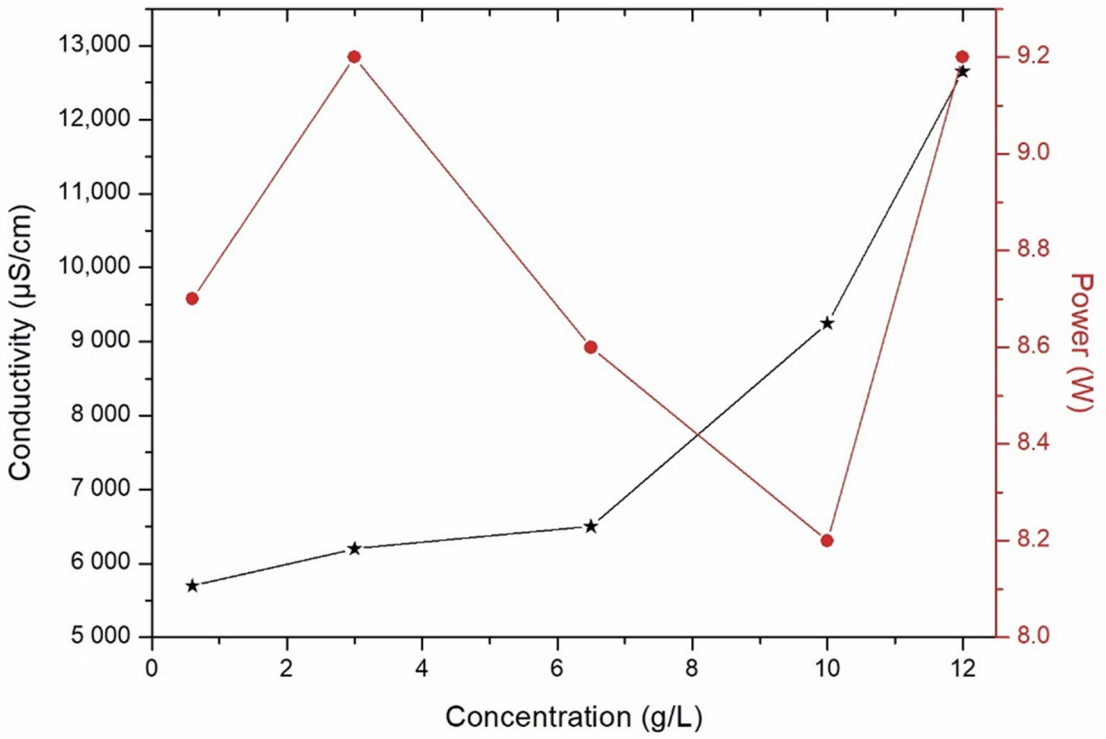


**Figure 2.** Conductivity and power consumed as a function of electrolyte concentration.

### *3.3. Morphological Analysis of the PEO Coating under the Best Condition*

The thin oxide coating was analyzed by Scanning Electron Microscopy (SEM) using a ZEISS EVO LS15 (Jena, Germany). Figure 3 presents the micrograph of the coating that exhibited the best energy consumption condition (Standard 5).

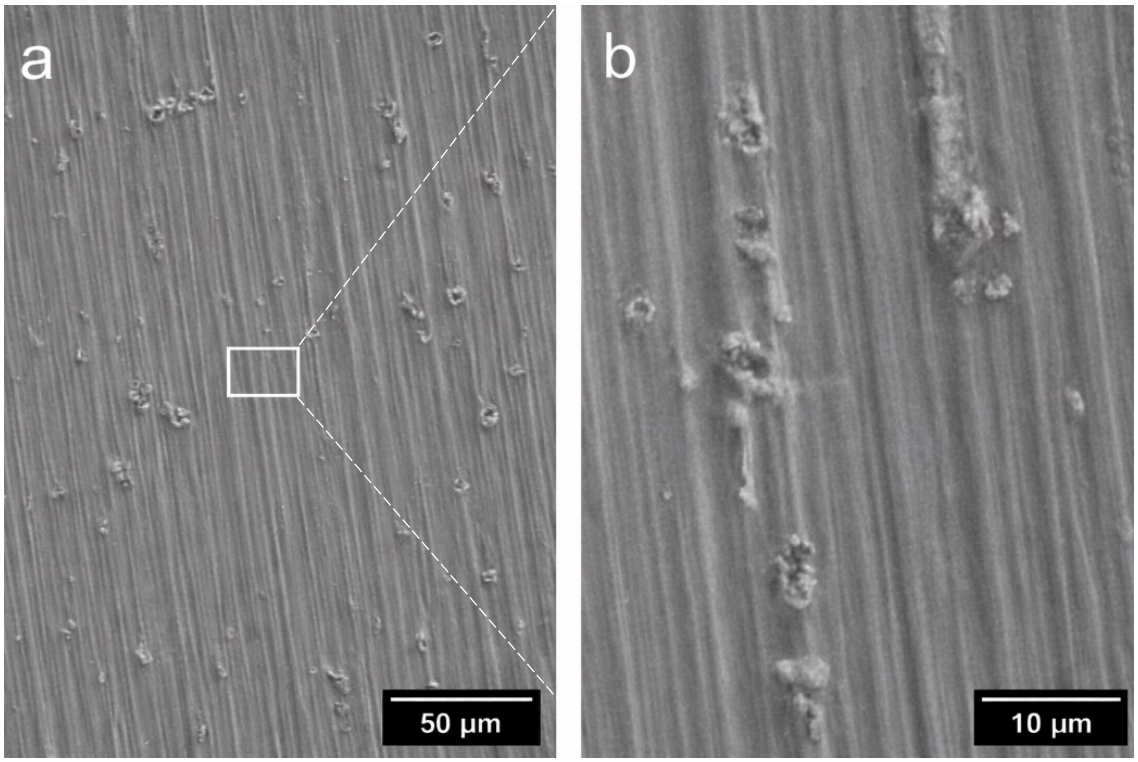


**Figure 3.** Scanning Electron Microscopy of the PEO coating (best condition) [17].

In the study by Lucas et al. [17], after the application of the PEO treatment, the resulting coating exhibited a morphology that significantly differs from PEO processes reported in the literature. Typically, PEO coatings are characterized by random protuberances along their surface, in addition to the presence of pores that arise due to the strong electric field formed on the samples, which causes not only electrical discharges but also the ejection of substrate elements into the coating [10,17].

In contrast, the coating in question demonstrated a highly compact structure, with a measured thickness of 1.0 ± 0.3 µm. The attributes of this coating can be attributed to the electrical regime employed, specifically a frequency of 25 kHz, which is known to induce an electron avalanche during the process, thereby facilitating rapid ionization and the generation of intense discharges, as illustrated in Figure 1.

This resulting high energy density, together with the electrolyte used, produces the minimal coating thickness, as evidenced in Figure 3, since the deposition process followed the orientation established by the previous grinding, resulting in the appearance of a “wave” pattern. Furthermore, the formation of small sealed pores is observed, although with reduced density.

### *3.4. Analysis of Variance (ANOVA) of Power Consumption Relative to the Parameters*

The analysis of variance (ANOVA) was used to assess the impact of interactions between various parameters on the response variable, specifically energy consumption. The adequacy of the model fit was evaluated using the coefficient of determination ($R^2$), which quantifies the proportion of overall variability in the process explained by the model. The minimum expected value for $R^2$ is approximately 80%; however, a value close to 100% indicates superior explanatory power of the model, thus denoting a more robust fit. In this study, the model accounted for approximately 89.86% of the total variability in the PEO process [18,24–26]. Table 4 presents the ANOVA analysis for this study.

**Table 4.** Analysis of variance (ANOVA) for the analyzed quadratic model.

| Source | DF | Sum of Square | *F*-Value | *p*-Value |
|---|---|---|---|---|
| Model | 9 | 131.65 | 6.90 | 0.0093 * |
| Time | 1 | 12.97 | 6.11 | 0.0427 * |
| Duty Cycle | 1 | 98.12 | 46.26 | 0.0003 * |
| Concentration | 1 | 0.34 | 0.16 | 0.7011 |
| Time$^2$ | 1 | 5.52 | 2.60 | 0.1506 |
| Duty Cycle$^2$ | 1 | 1.35 | 0.64 | 0.4516 |
| Concentration$^2$ | 1 | 0.28 | 0.13 | 0.7269 |
| Time x Duty Cycle | 1 | 10.30 | 4.85 | 0.0634 |
| Time x Concentration | 1 | 1.65 | 0.78 | 0.4074 |
| Duty Cycle x Concentration | 1 | $1.25 \times 10^{-5}$ | $5.89 \times 10^{-6}$ | 0.9981 |
| Lack of Fit | 5 | 10.07 | 0.84 | 0.6208 |
| Pure Error | 2 | 4.77 | | |
| $R^2$ | | 89.86% | | |

* Significant factor for the statistical model.

In Table 4, the *p*-value is crucial because it allows us to determine if the corresponding factor is significant ($p < 0.05$). When this criterion is met, it indicates that the model provides at least 95% confidence [26].

The significance of treatment time and duty cycle in the PEO process is demonstrated by their *p*-values being less than 0.05, indicating a significant impact on power consumption. Conversely, the electrolyte concentration factor did not show statistical significance in power consumption. However, as seen in Table 3, increasing electrolyte concentration does affect power consumption by enhancing the conductivity of the electrolyte and facilitating ion transfer. The very low *F*-value for the "Concentration" factor suggests a possibility of noise around 70.11%. This finding is supported by another study investigating the effects of these parameters in the PEO process for other applications [16].

The *F*-value of 6.90 indicates that the model is statistically significant, suggesting that the probability of this value arising by chance (noise) is only 0.93%. This low probability reinforces the model's reliability in explaining the variance in the data, with the sole exception of the "concentration" factor [16,25,26].

To evaluate the influence of each independent variable on the dependent variable, Equation (2), which is designated as the effect size ($\eta^2$), may be employed. This equation integrates the sum of squares attributable to factors, blocks, and/or the statistical model itself to measure the variability inherent within a data set [16,26].

$$\eta^2 = \frac{SS}{SST} \times 100 \tag{2}$$

Where "*SS*" denotes the sum of squares corresponding to a specific factor, serving as a metric for the variability attributed to that factor within the statistical framework, while "*SST*" represents the total sum of squares of the model, encompassing all observed variability in the data set, considering both explanatory variables and associated errors. Based on the application of Equation (2), it is observed that the parameters with the greatest influence on power consumption are Duty Cycle (66.98%), treatment time (8.85%), and electrolyte concentration (0.23%). The lack of fit and pure error of the model account for approximately 10.13% of the total variability, a relatively high value indicating the need for further studies to assess these factors in greater detail.

Once the significance of the model for the response variable has been verified, a linear regression can be performed to estimate the parameters relevant to the PEO process that have been optimized. Since the "concentration" factor did not show significance in the response variable, it was removed from the equation. The regression is outlined in Equation (3).

$$\begin{aligned} \text{Power } (W) = {} & -9.64235 + (0.041746 \times \text{Time}) + (0.31193 \times \text{Duty Cycle}) \\ & - (3.03 \times 10^{-5} \times \text{Time}^2) - (6.54 \times 10^{-4} \times \text{Duty Cycle}^2) \\ & - (3.03 \times 10^{-4} \times \text{Time} \times \text{Duty Cycle}) \end{aligned} \tag{3}$$

The predicted values, compared with the empirical values, were analyzed using the response variable "power" (*W*), as shown in Figure 4a. The observed data points display a linear correlation with a certain degree of dispersion, which can be attributed to the complex interaction between the examined parameters (treatment time and Duty Cycle). A contour plot was generated using Design-Expert software to determine the minimum average power used, as illustrated in Figure 4b. The estimated minimum power value was determined to be 3.60 Watts, considering the establishment and maintenance of the plasma over a time interval. For this purpose, the software outlined the experimental parameters, which are detailed in Table 5.

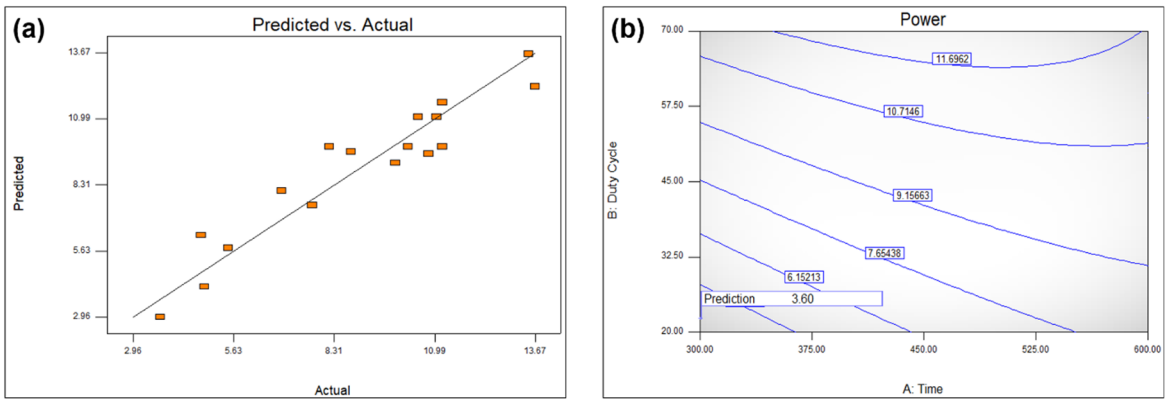


**Figure 4.** (**a**) Graph of predicted vs. actual values; (**b**) Contour plot for power consumption.

**Table 5.** Parameters to minimize power consumption in the PEO process.

| Solution | Time (s) | Duty Cycle (%) | Power (W) | Desirability |
|---|---|---|---|---|
| 01 | 300 | 20 | 3.93 | 0.975 |
| 02 | 300 | 20 | 4.16 | 0.952 |
| 03 | 300 | 20 | 4.21 | 0.947 |
| 04 | 597 | 20 | 7.49 | 0.618 |
| 05 | 571 | 20 | 7.82 | 0.585 |

In Table 5, alongside the significant parameters and the predicted power consumption, the "Desirability" function has been incorporated. This function evaluates the degree to which a specific combination of variables (treatment time and Duty Cycle) can achieve a predetermined power target. Desirability values range from 0 to 1, where 0 means that one or multiple variables do not meet the target, while 1 indicates an optimal system that completely fulfils the specified objective, thus facilitating a thorough assessment of optimal solutions in multi-response scenarios [27–29]. In the present investigation, it has been noted that solutions 01, 02, and 03 effectively satisfy the power objectives established by the software, exhibiting values that are remarkably close to 1.0.

## 4. Conclusions

This study applied a Central Composite Design (CCD) to statistically investigate the influence of treatment time, duty cycle, and electrolyte concentration on the average power consumption during the Plasma Electrolytic Oxidation (PEO) process on AA2024 aluminum alloy. The analysis of the electrical behavior throughout the treatment revealed the three typical stages of the PEO process: anodic oxidation, spark discharge, and micro-arc oxidation, the latter being essential for the growth and adhesion of the oxide coating to the substrate.

The average power consumption ranged from 3.68 W to 13.67 W, with the lowest values associated with shorter treatment times and lower duty cycle values. The ANOVA results confirmed the statistical significance of the model, which explained 89.86% of the data variability. Among the evaluated parameters, duty cycle (66.98%) and treatment time (8.85%) were identified as the most influential factors affecting the process energy consumption. Although the electrolyte concentration did not show statistical significance in the model, it still plays an important role in the electrochemical environment, influencing solution conductivity, charge transport, and the stability of plasma discharges.

Response surface optimization indicated that the conditions of 300 s treatment time and 20% duty cycle can reduce the average power consumption to approximately 3.92 W, with a desirability of 0.975, representing an energetically optimized operating condition for the PEO process.

The morphological analysis by Scanning Electron Microscopy (SEM) of the sample produced under the lowest energy consumption condition revealed the formation of a compact oxide coating with an approximate thickness of 1.0 ± 0.3 μm. Unlike many PEO coatings reported in the literature, which often present high surface roughness and a large density of open pores, the obtained layer exhibited a relatively uniform morphology with a low density of sealed pores, with features partially influenced by the initial surface preparation of the sample. This behavior can be associated with the applied electrical regime (25 kHz), which promotes rapid and intense micro-discharges, affecting the coating growth mechanism.

Overall, the results demonstrate that applying statistical methods to analyze and optimize operational parameters can significantly reduce energy consumption in the PEO process without compromising coating formation, thereby contributing to the development of more efficient and sustainable surface treatments.

Furthermore, the findings provide a scientific basis for future investigations involving additional process parameters, such as electrode spacing, electrolyte temperature, and the use of electrolyte additives, aiming at further optimization of plasma electrolytic oxidation for industrial applications.

## Author Contributions

R.R.L.: writing—revision and editing, writing—original draft, methodology, investigation, formal analysis, data curation, conceptualization. R.P.M.: writing—revision and editing, investigation, supervision, resources, funding acquisition. E.C.B.: writing—revision and editing, visualization, validation. R.d.C.M.S.-C.: writing—revision and editing, visualization, validation. All authors have read and agreed to the published version of the manuscript.

## Funding

This research was funded by the Coordination for the Improvement of Higher Education Personnel (CAPES) through process no. 88881.933644/2024-1, and received a scholarship from the São Paulo Research Foundation (FAPESP) under process no. 2023/07918-5.

## Institutional Review Board Statement

Not applicable.

## Informed Consent Statement

Not applicable.

## Data Availability Statement

Not applicable.

## Acknowledgments

The authors would like to thank the Technical Engineer Miguel de Omena Lucas for all the technical support.

## Conflicts of Interest

The authors declare no conflict of interest.

## Use of AI and AI-Assisted Technologies

During the preparation of this work, the authors used ChatGPT to improve their writing. After using this tool, the authors reviewed and edited the content as needed and assume full responsibility for the content of the published article.

## References

1. Rawart, S.; Wang, C.; Lay, S.; et al. Sustainable Biochar for Advanced Electrochemical/Energy Storage Applications. *J. Energy Storage* **2023**, *63*, 107115. https://doi.org/10.1016/j.est.2023.107115.
2. Baruch-Mordo, S.; Kiesecker, J.; Kennedy, C.; et al. From Paris to Practice: Sustainable Implementation of Renewable Energy Goals. *Environ. Res. Lett.* **2019**, *14*, 024013. https://doi.org/10.1088/1748-9326/aaf6e0.
3. Rivera-Cerezo, H.; Gaona-Tiburcio, C.; Cabral-Miramontes, J.; et al. Effect of Heat Treatment on the Electrochemical Behavior of AA2055 and AA2024 Alloys for Aeronautical Applications. *Metals* **2023**, *13*, 429. https://doi.org/10.3390/met13020429.
4. Aamir, M.; Giasin, K.; Tolouei-Rad, M.; et al. A Review: Drilling Performance and Hole Quality of Aluminium Alloys for Aerospace Applications. *J. Mater. Res. Technol.* **2020**, *9*, 12484–12500. https://doi.org/10.1016/j.jmrt.2020.09.003.
5. Anijdan, S.; Sadeghi-Nezhad, D.; Lee, H.; et al. TEM Study of S' Hardening Precipitates in the Cold Rolled and Aged AA2024 Aluminum Alloy: Influence on the Microstructural Evolution, Tensile Properties & Electrical Conductivity. *J. Mater. Res. Technol.* **2021**, *13*, 798–807. https://doi.org/10.1016/j.jmrt.2021.05.003.
6. Zhu, L.; Li, N.; Childs, P. Light-Weighting in Aerospace Component and System Design. *Propuls. Power Res.* **2018**, *7*, 103–119. https://doi.org/10.1016/j.jppr.2018.04.001.
7. Tomczyk, K.; Stepniowski, W. Incorporation of Anions into Anodic Alumina—A New Track in Cr(VI) Anodizing Substitution? *Materials* **2024**, *17*, 2938. https://doi.org/10.3390/ma17122938.

8. Godja, N.; Munteanu, F. Environmentally Friendly Solutions as Potential Alternatives to Chromium-Based Anodization and Chromate Sealing for Aeronautic Applications. *Coatings* **2025**, *15*, 439. https://doi.org/10.3390/coatings15040439.
9. Hou, F.; Gorthy, R.; Mardon, I.; et al. Low Voltage Environmentally Friendly Plasma Electrolytic Oxidation Process for Titanium Alloys. *Sci. Rep.* **2022**, *12*, 6037. https://doi.org/10.1038/s41598-022-09693-w.
10. Lucas, R.; Sales-Contini, R.; Silva, F.; et al. Plasma Electrolytic Oxidation (PEO): An Alternative to Conventional Anodization Process. *AIMS Mater. Sci.* **2024**, *11*, 684–711. https://doi.org/10.3934/matersci.2024035.
11. Lucas, R.; Hein, L.; Botelho, E.; et al. Influence of Electrolyte Concentration Variation on Thin Oxide Coating Production in Aluminum Alloy by PEO. *Trans. Indian Natl. Acad. Eng.* **2024**, *9*, 979–986. https://doi.org/10.1007/s41403-024-00500-8.
12. Marcuz, N.; Ribeiro, R.; Rangel, E.; et al. Exploiting the Effect of PEO Parameters on the Surface of AISI 1020 Low-Carbon Steel Treated in a TaOH-Rich Electrolyte. *Surf. Coat. Technol.* **2024**, *477*, 130374. https://doi.org/10.1016/j.surfcoat.2024.130374.
13. Cheng, Y.; Wei, B.; Liu, Y.; et al. Plasma Electrolytic Oxidation of Copper in an Aluminate Based Electrolyte with the Respective Additives of $Na_3PO_4$, $NaH_2PO_4$ and $NaH_2PO_2$. *Appl. Surf. Sci.* **2021**, *565*, 150477. https://doi.org/10.1016/j.apsusc.2021.150477.
14. Guo, F.; Cao, Y.; Wang, K.; et al. Effect of the Anodizing Temperature on Microstructure and Tribological Properties of 6061 Aluminum Alloy Anodic Oxide Films. *Coatings* **2022**, *12*, 314. https://doi.org/10.3390/coatings12030314.
15. Matykina, E.; Arrabal, R.; Pardo, R.; et al. Energy-Efficient PEO Process of Aluminium Alloys. *Mater. Lett.* **2014**, *127*, 13–16. https://doi.org/10.1016/j.matlet.2014.04.077.
16. Troughton, S.; Nominé, A.; Henrion, G.; et al. Synchronised Electrical Monitoring and High Speed Video of Bubble Growth Associated with Individual Discharges during Plasma Electrolytic Oxidation. *Appl. Surf. Sci.* **2015**, *359*, 405–411. https://doi.org/10.1016/j.apsusc.2015.10.124.
17. Lucas, R.; Silva, E.; Marques, L.; et al. Analysis of Plasma Electrolytic Oxidation Process Parameters for Optimizing Adhesion in Aluminum–Composite Hybrid Structures. *Appl. Sci.* **2024**, *14*, 7972. https://doi.org/10.3390/app14177972.
18. Dehnavi, V.; Luan, B.; Shoesmith, D.; et al. Effect of Duty Cycle and Applied Current Frequency on Plasma Electrolytic Oxidation (PEO) Coating Growth Behavior. *Surf. Coat. Technol.* **2013**, *226*, 100–107. https://doi.org/10.1016/j.surfcoat.2013.03.041.
19. Zhu, M.; Song, K.; Dong, D.; et al. Correlation between the Transient Variation in Positive/Negative Pulse Voltages and the Growth of PEO Coating on 7075 Aluminum Alloy. *Electrochim. Acta* **2022**, *411*, 140056. https://doi.org/10.1016/j.electacta.2022.140056.
20. Sevidova, E.; Pupan, L.; Gutsalenko, Y.; et al. Effect of Morphological Features on Dielectric Properties of Plasma Electrolytic Oxidation Coatings on D16T Aluminum Alloy. In *Advances in Design, Simulation and Manufacturing III, Proceedings of the 3rd International Conference on Design, Simulation, Manufacturing: The Innovation Exchange, DSMIE-2020, Kharkiv, Ukraine, 9–12 June 2020*; Springer: Berlin/Heidelberg, Germany, 2020; pp. 542–551. https://doi.org/10.1007/978-3-030-50794-7_53.
21. Francisca, G.S.O.; Vitoriano, J.O.; Alves-Junior, C. Controlling Plasma Electrolytic Oxidation of Titanium Using Current Pulses Compatible with the Duration of Microdischarges. *Results Mater.* **2022**, *15*, 100310. https://doi.org/10.1016/j.rinma.2022.100310.
22. Tavares, M.; Vitoriano, J.; Silva, R.; et al. Effect of Duty Cycle and Treatment Time on Electrolytic Plasma Oxidation of Commercially Pure Al Samples. *J. Mater. Res. Technol.* **2019**, *8*, 2141–2147. https://doi.org/10.1016/j.jmrt.2019.01.020.
23. Yan, H.; Liu, W.; Ma, Y.; et al. Effects of Micro-Arc Oxidation Process Parameters on Microstructure and Properties of $Al_2O_3$ Coatings Prepared on Sintered 2024 Aluminum Alloy. *J. Mater. Eng. Perform.* **2024**, *33*, 1862–1873. https://doi.org/10.1007/s11665-023-08093-z.
24. Zhang, X.; Tian, X.; Yang, S.; et al. Low Energy-Consumption Plasma Electrolytic Oxidation Based on Grid Cathode. *Rev. Sci. Instrum.* **2010**, *81*, 103504. https://doi.org/10.1063/1.3500319.
25. Bahador, R.; Hosseinabadi, N.; Yaghtin, A. Effect of Power Duty Cycle on Plasma Electrolytic Oxidation of A356–$Nb_2O_5$ Metal Matrix Composites. *J. Mater. Eng. Perform.* **2021**, *30*, 2586–2604. https://doi.org/10.1007/s11665-021-05597-4.
26. Kroes, A.; Finley, J. Demystifying Omega Squared: Practical Guidance for Effect Size in Common Analysis of Variance Designs. *Psychol. Methods* **2023**, *30*, 866–887. https://doi.org/10.1037/met0000581.
27. Chaharmahali, R.; Fattah-alhosseini, A.; Karbasi, M.; et al. A Systematic Study on Modulation of Plasma Electrolytic Oxidation Parameters for Optimizing Photocatalytic Coatings on Titanium Substrates. *J. Alloys Compd.* **2023**, *963*, 171234. https://doi.org/10.1016/j.jallcom.2023.171234.
28. Torres-Cerón, D.; Restrepo-Parra, E.; Acosta-Medina, C.; et al. Study of Duty Cycle Influence on the Band Gap Energy of $TiO_2$/P Coatings Obtained by PEO Process. *Surf. Coat. Technol.* **2019**, *375*, 221–228. https://doi.org/10.1016/j.surfcoat.2019.06.021.
29. Costa, N.; Lourenço, J. Desirability-Based Post-Hoc Selection of Pareto Solutions. *Int. J. Manag. Sci. Eng. Manag.* **2024**, *19*, 251–260. https://doi.org/10.1080/17509653.2023.2296876.